Calculation of Relative Binding Free Energy Differences for Fructose 1,6-Bisphosphatase Inhibitors Using the Thermodynamic Cycle Perturbation Approach

M. Rami Reddy* and Mark D. Erion*

Contribution from Metabasis Therapeutics, Inc., 9390 Towne Centre Drive, San Diego, California 92121

Received February 6, 2001. Revised Manuscript Received April 2, 2001

Abstract: An iterative, computer-assisted, drug design strategy that combines molecular design, molecular mechanics, molecular dynamics (MD), and free energy perturbation (FEP) calculations with compound synthesis, biochemical testing of inhibitors, and crystallographic structure determination of protein−inhibitor complexes was successfully used to predict the rank order of a series of nucleoside monophosphate analogues as fructose 1,6-bisphosphatase (FBPase) inhibitors. The X-ray structure of FBPase complexed with 5-aminoimidazole-4-carboxamide-1-β-D-ribofuranosyl 5′-monophosphate (ZMP) provided structural information used for subsequent analogue design and free energy calculations. The FEP protocol was validated by calculating the free energy differences for the mutation of ZMP (**1**) to AMP (**2**). The calculated results showed a net gain of 1.7 kcal/mol, which agreed with the experimental result of 1.3 kcal/mol. FEP calculations were performed for 18 other AMP analogues. Inhibition constants were determined for over half of these analogues, usually after completion of the calculation, and were consistent with the predictions. Solvation free energy differences between AMP and various AMP analogues proved to be an important factor in binding free energies, suggesting that increased desolvation costs associated with the addition of polar groups to an inhibitor must be overcome by stronger ligand−protein interactions if the structural modification is to enhance inhibitor potency. The results indicate that FEP calculations predict relative binding affinities with high accuracy and provide valuable insight into the factors that influence inhibitor binding and therefore should greatly aid efforts to optimize initial lead compounds and reduce the time required for the discovery of new drug candidates.

Introduction

Computer-assisted drug design (CADD) has contributed to the successful discovery of numerous novel enzyme inhibitors, including inhibitors of thymidylate synthase, HIV-1 protease, and purine nucleoside phosphorylase.[1] In each case, CADD was used to predict the relative binding affinity of an inhibitor designed from a lead compound prior to synthesis. A free energy simulation technique known as the thermodynamic cycle perturbation (TCP) approach[2] used in conjunction with molecular dynamics calculations offers a theoretically precise method of determining the binding free energy differences of structurally related inhibitors. Despite its high accuracy, free energy calculations[3] have primarily been used to rationalize experimentally determined binding affinities rather than predict affinities of new analogues. The reluctance to use free energy calculations for predictions and therefore drug design is partly related to its large CPU requirements and its limited use for the evaluation of large sets of compounds or compounds that differ significantly in structure from the lead compound. Nevertheless, a few studies have reported promising results using the TCP approach.[4] For example, HIV-1 protease inhibitors were

* Correspondence may be addressed to either author. E-mail: reddy@mbasis.com or erion@mbasis.com.

(1) (a) Appelt, K.; Bacquet, R. J.; Bartlett, C. A.; Booth, C. L.; Freer, S. T.; Fuhry, M. A.; Gehring, M. R.; Hermann, S. M.; Howland, E. F.; Janson, C. A.; Jones, T. R.; Kan, C.; Kathardekar, V.; Lewis, K. K.; Marzoni, G. P.; Matthews, D. A.; Mohr, C.; Moomaw, E. W.; Morse, C. A.; Oatley, S. J.; Ogden, R. O.; Reddy, M. R.; Reich, S. H.; Schoettlin, W. S.; Smith, W. W.; Varney M. D.; Villafranca, J. E.; Ward, R. W.; Webber, S.; Webber, S. E.; Welsh, K. M.; White, J. *J. Med. Chem.* **1991**, *34*, 1925−1934. (b) Holloway, K.; Wai, J. M.; Halgren, T. A.; Fitzgerald, P. M.; Vacca, J.; Dorsey, B. D.; Levin, R. B.; Thompson, W. J.; Chen, J. L.; deSolms, J. S.; Gaffin, N.; Ghosh, A. K.; Giuliani, E. A.; Graham, S. L.; Guare, J. P.; Hungate, R. W.; Lyle, T. A.; Sanders, W. M.; Tucker, T. J.; Wiggins, M.; Wiscount, C. M.; Woltersdorf, O. W.; Young, S. D.; Darke, P. L.; Zugay, J. A. *J. Med. Chem.* **1995**, *38*, 305−317. (c) Varney, M. D.; Appelt, K.; Kalish, V.; Reddy, M. R.; Tatlock, J.; Palmer, C. L.; Romies, W. H.; Wu, B. W.; Musick, L. *J. Med. Chem.* **1994**, *37*, 2274−2284. (d) Montgomery, J. A.; Niwas, S.; Rose, J. D.; Secrist, J. A.; Sudhakar Babu, Y.; Bugg, C. E.; Erion, M. D.; Guida, W. C.; Ealick, S. E. *J. Med. Chem.* **1993**, *36*, 55−69. (e) Reddy, M. R.; Parrill, A. In *Rational Drug Design: Novel Methodology and Practical Applications*; Parrill, A., Reddy, M. R., Eds.; ACS Symposium Series 719; Oxford University Press: Washington, DC, 1999; pp 1−11.

(2) (a) Beveridge, D. L.; DiCapua, F. M. *Annu. Rev. Biophys. Biophys. Chem.* **1989**, *18*, 431−492. (b) McCammon, J. A. *Curr. Opin. Struct. Biol.* **1991**, *1*, 196−200. (c) *Molecular Dynamics and Protein Structure*; Hermans, J., Ed.; Polycrystal: West Springs, IL, 1985. (d) Rami, M. R.; Bacquet, R. J.; Zichi, D.; Matthews, D. A.; Welsh, K. M.; Jones, T. R.; Freer, S. *J. Am. Chem. Soc.* **1992**, *114*, 10117−10122. (e) Gao, J.; Kuczera, K.; Tidor, B.; Karplus, M. *Science* **1989**, *244*, 1069−1072.

(3) (a) Reddy, M. R.; Erion, M. D.; Agarwal, A. In *Reviews in Computational Chemistry*; Lipkowitz, K. B., Boyd, D. B, Eds.; Wiley: New York, 2000; Vol. 2, pp 217−304. (b) Reddy, M. R.; Viswanadhan, V. N.; Weinstein, J. N. *Proc. Natl. Acad. Sci. U.S.A.* **1991**, *88*, 10287−10291. (c) Ferguson, D. M.; Radmer, R. J.; Kollman, P. A. *J. Med. Chem.* **1991**, *34*, 2654−2659. (d) Tropshaw, A. J.; Hermans, J. *Protein Eng.* **1992**, *5*, 29−33. (e) Rao, B. G.; Tilton, R. F.; Singh, U. C. *J. Am. Chem. Soc.* **1992**, *114*, 4447−4452. (f) Erion, M. D.; Reddy, M. R. *J. Am. Chem. Soc.* **1998**, *120*, 3295−3304.

(4) (a) Merz, K. M.; Kollman, P. A. *J. Am. Chem. Soc.* **1989**, *111*, 5649−5658. (b) Reddy, M. R.; Varney, M. D.; Kalish, V.; Viswanadhan, V. N.; Appelt, K. *J. Med. Chem.* **1994**, *37*, 1145−1152.

10.1021/ja0103288 CCC: $20.00
Published on Web 06/07/2001

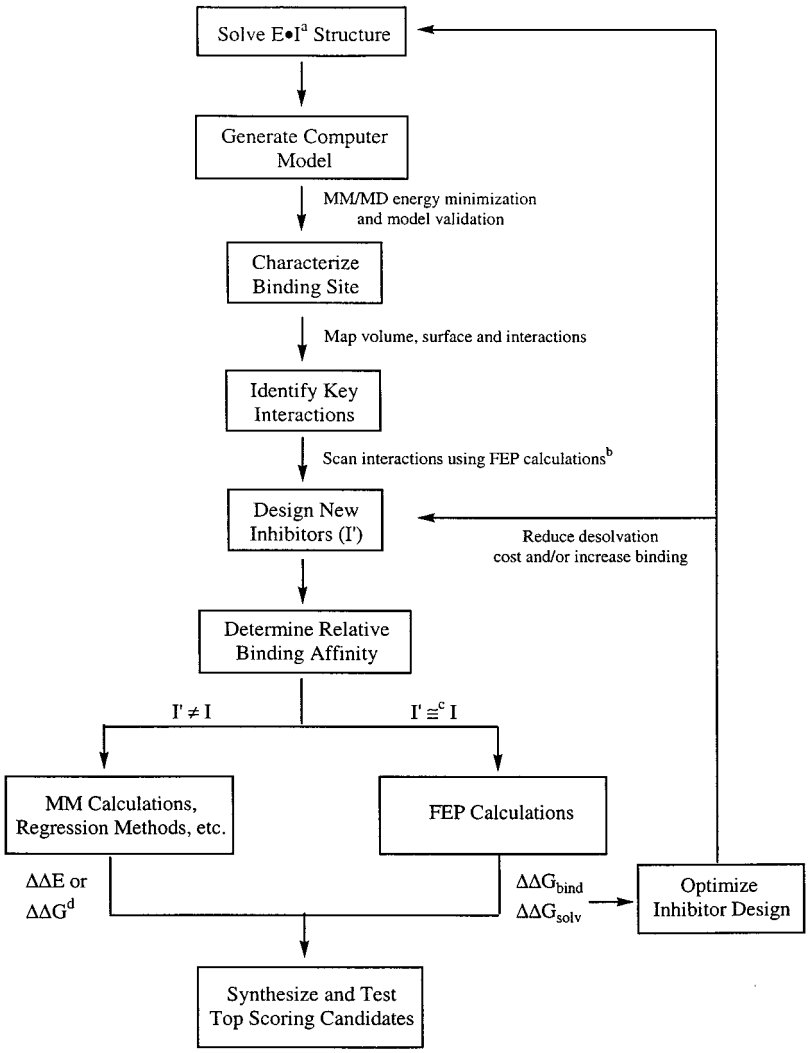

Figure 1. CADD flowchart. [a] E•I = enzyme−inhibitor complex. [b] Scan binding interactions using strategy described in ref 5. [c] I and I′ are structurally similar. [d] Relative energies or estimated relative free energies.

successfully optimized using TCP calculations as part of an iterative structure-based design study.[4b] More recently,[5] the contributions of individual heteroatoms of adenosine monophosphate (AMP) to fructose 1,6-bisphosphatase binding affinity were successfully rank ordered using the free energy perturbation (FEP) methodology. Fructose 1,6-bisphosphatase (FBPase) is a potential target for type II diabetes drugs based on its central role within the gluconeogenesis pathway[6] and the association of this pathway with the excessive production of glucose by the livers of non-insulin-dependent diabetes mellitus patients.[7] AMP inhibits FBPase activity by binding to an allosteric site and inducing a conformational change. The present article describes our efforts to predict the SAR of AMP analogues by calculating the relative solvation and binding free energies with the hope that this information would ultimately aid the discovery of potent FBPase inhibitors using the iterative process described in Figure 1.

Methods

Computer-Aided Drug Design Scheme. High-resolution X-ray structures of human FBPase inhibitor complexes were used to study the interactions of potential ligands with the FBPase allosteric binding site.[8] Newly designed analogues were docked in the AMP binding site and examined individually. The most promising analogues were selected for further calculations on the basis of their interactions with the binding-site residues. The relative binding affinities were calculated using the free energy perturbation method, and the analogues exhibiting significantly enhanced binding affinities were synthesized and evaluated as FBPase inhibitors.

Thermodynamic Cycle−Perturbation (TCP) Approach. Thermodynamic cycle perturbation is a method that computes the relative change in binding free energy through nonphysical paths connecting the desired initial and terminal states.[9] This approach enables calculation of the relative change in binding free energy ($\Delta\Delta G_{bind}$) between two related compounds by computationally simulating the "mutation" of one to the other. The relative solvation free energy change for the two

(5) Erion, M. D.; van Poelje, P. D.; Reddy, M. R. *J. Am. Chem. Soc.* **2000**, *122*, 6114−6115.

(6) Granner, D.; Pilkis, S. J. *J. Biol. Chem.* **1990**, *265*, 10173−10176.

(7) (a) Rothman, D. L.; Magnusson, I.; Katz, L. D.; Shulman, R. G.; Shulman, G. I. *Science* **1991**, *254*, 573−576. (b) Magnusson, I.; Rothman, D. L.; Katz, L. D.; Shulman, R. G.; Shulman, G. I. *J. Clin. Invest.* **1992**, *90*, 1323−1327.

(8) (a) Ke, H. M.; Zhang, Y. P.; Lipscomb, W. N. *Proc. Natl. Acad. Sci. U.S.A.* **1990**, *87*, 5243−5247. (b) Iversen, L. F.; Brzozowski, M.; Hastrup, S.; Hubbard, R.; Kastrup, J. S.; Larsen, I. K.; Naerum, L.; Norskov-Lauridsen, L.; Rasmussen, P. B.; Thim, L.; Wiberg, F. C.; Lundgren, K. *Protein Sci.* **1997**, *6*, 971−982.

(9) (a) Zwanzig, R. J. *J. Chem. Phys.* **1954**, *22*, 1420. (b) Beveridge, D. L.; DiCapua, F. M. *Annu. Rev. Biophys. Biophys. Chem.* **1989**, *18*, 431. (c) Bash, P. A.; Singh, U. C.; Brown, F. K.; Langridge, R.; Kollman, P. A. *Science* **1987**, *235*, 574−576.

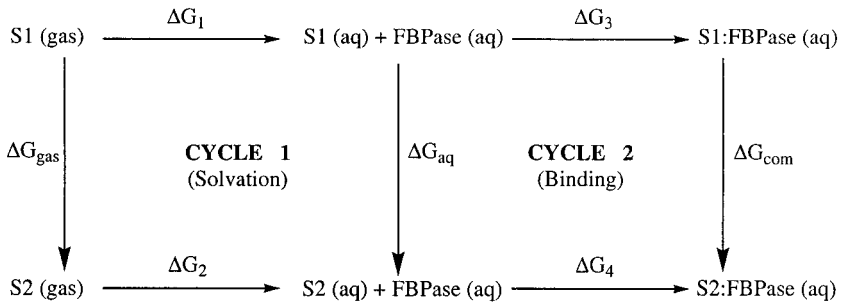

Figure 2. Thermodynamic cycles used to calculate the relative solvation free energy (cycle 1) and relative binding free energy (cycle 2).

ligands is computed using the first part of cycle shown in Figure 2 and represented in eq 1:

$$\Delta G_2 - \Delta G_1 = \Delta G_{aq} - \Delta G_{gas} = \Delta\Delta G_{sol} \quad (1)$$

The relative binding free energy change for the two ligands is computed using the second part of the cycle shown in Figure 2 and represented by eq 2:

$$-k_B T \ln(k2/k1) = \Delta G_4 - \Delta G_3 = \Delta G_{com} - \Delta G_{aq} = \Delta\Delta G_{bind} \quad (2)$$

where k_B is the Boltzmann constant, T is the absolute temperature, and $k1$ and $k2$ refer to the experimentally measured binding constants for inhibitors S1 and S2, respectively, and ΔG_3 and ΔG_4 to the corresponding free energy differences.

The free energy change for converting molecule S1 into molecule S2 is computed by perturbing the Hamiltonian of reactant S1 (initial state) into product S2 (final state). This transformation is accomplished through a parametrization of terms comprising the interaction potentials of the system with a change of state variable that maps onto reactant and product states when that variable is 0 and 1, respectively. The total free energy change for the mutation from the initial to the final state is computed by summing "incremental" free energy changes over several windows visited by the state variable as it changes from 0 to 1.

Single and Double Topology Methods. The single topology method entails changing the appropriate reactant atoms to product atoms. The mutation often results in geometrical changes as well as changes in partial charges and van der Waals parameters. Prior to the mutation, the system was minimized using 500 steps of steepest descent and 2000 steps of conjugate gradient and then equilibrated for 20 ps. Each mutation was then completed using 101 windows, with each window comprising 1 ps of equilibration and 2 ps of data collection or 303 ps of total MD simulation.

In the double topology or thread method,[10] a single topology is defined for those atoms that are identical in both molecules (i.e. force constants and equilibrium geometries are the same but partial charges can vary). For the portion of the molecule which is transformed, both the starting (reactant) and ending (product) topologies are defined using their associated geometries, with one beginning and the other ending the simulation entirely as dummy atoms. Dummy atoms are identical to real atoms except that their Lennard-Jones parameters and charges are set to zero. At intermediate points during the transformation, all atoms in both topologies have fractional Lennard-Jones parameters and charges. Additionally, molecules with both topologies interact with the environment but not with each other.

In each mutation, the system was initially minimized using 500 steps of steepest descent and 2000 steps of conjugate gradient and then equilibrated for 20 ps. A two-stage procedure was used to obtain relative free energy differences from the molecular dynamics simulations. During the first stage, the charges of the reactant atoms are turned off while the Lennard-Jones parameters of the product atoms are turned on. During the second stage, the Lennard-Jones parameters of the reactant atoms are turned off while the charges of the product atoms are turned on. This procedure has been used previously[10] to achieve convergence. Each stage of the simulation was performed using 101 windows with each window comprising 1 ps of equilibration and 2 ps of data collection. Thus, a molecular dynamics simulation of 626 ps run was used for each mutation. Previous studies suggest that shorter simulations are often associated with convergence problems with the thread method.[10]

Convergence or Statistical Error Estimation. A doublewide sampling procedure was followed for all of the mutations, and the reported results are based on the averages from the backward and forward simulations. Convergence was tested by comparing the relative change in the free energy for the AMP-to-ZMP mutation using two different lengths of molecular dynamics simulations. Errors were estimated for each window by dividing the window statistics into four groups (in both forward and backward directions) and computing the standard deviation for the indicated free energy change. The root mean square of these window errors is reported as a measure of the statistical uncertainty in the calculation.

Computational Details

All molecular dynamics, molecular mechanics, and FEP calculations were carried out with the AMBER program using an all atom force field[11] and the SPC/E model potential[12] to describe water interactions. Electrostatic charges and parameters for the standard residues were taken from the AMBER database. For nonstandard solute atoms, partial charges were obtained by fitting wave functions calculated with Gaussian94[13] at the 6-31G* basis set level with CHELP.[14] All equilibrium bond lengths, bond angles, and dihedral angles for nonstandard residues were taken from ab initio optimized geometries. Missing force field parameters were estimated from similar chemical species within the AMBER database. Parameters and partial atomic charges for all of the inhibitors and calculated relative gas, aqueous, and complex free energies between AMP and its analogues are available in the Supporting Information.

Solvation free energies were computed (the first cycle of Figure 2) by solvating the solute with SPC/E water using the AMBER box option. All of the water molecules located greater

(10) (a) Singh, U. C. *Proc. Natl. Acad. Sci. U.S.A.* **1988**, *85*, 4280. (b) Reddy, M. R.; Bacquet, R. J.; Zichi, D.; Matthews, D. A.; Welsh, K. M.; Jones, T. R.; Freer, S. *J. Am. Chem. Soc.* **1992**, *114*, 10117.

(11) (a) Weiner, S. J.; Kollman, P. A.; Case, D. A.; Singh, U. C.; Ghio, C.; Alagoha, G.; Profeta, S., Jr.; Weiner, P. K. *J. Am. Chem. Soc.* **1984**, *106*, 765−784. (b) Singh, U. C.; Weiner, P. K.; Caldwell, J. K.; Kollman, P. A. *AMBER Version 3.0*; University of California at San Francisco: San Francisco, 1986.

(12) (a) Berendsen, H. J. C.; Grigera, J. R.; Straatsma, T. P. *J. Phys. Chem.* **1987**, *91*, 6269−6271. (b) Reddy, M. R.; Berkowitz, M. *Chem. Phys. Lett.* **1989**, *155*, 173−176.

(13) Frisch, M. J.; Trucks, G. W.; Schlegel, H. B.; Gill, P. M. W.; Johnson, B. G.; Robb, M. A.; Cheeseman, J. R.; Keith, T.; Petersson, G. A.; Montgomery, J. A.; Raghavachari, K.; Al-Laham, M. A.; Zakrzewski, V. G.; Ortiz, J. V.; Foresman, J. B.; Cioslowski, J.; Stefanov, B. B.; Nanayakkara, A.; Challacombe, M.; Peng, C. Y.; Ayala, P. Y.; Chen, W.; Wong, M. W.; Andres, J. L.; Replogle, E. S.; Gomperts, R.; Martin, R. L.; Fox, D. J.; Binkley, J. S.; Defrees, D. J.; Baker, J.; Stewart, J. P.; Head-Gordon, M.; Gonzalez, C.; Pople, J. A. *Gaussian 94*; Gaussian, Inc.: Pittsburgh, PA, 1995.

(14) Chirlian, L. E.; Francl, M. M. *J. Comput. Chem.* **1987**, *8*, 894−905.

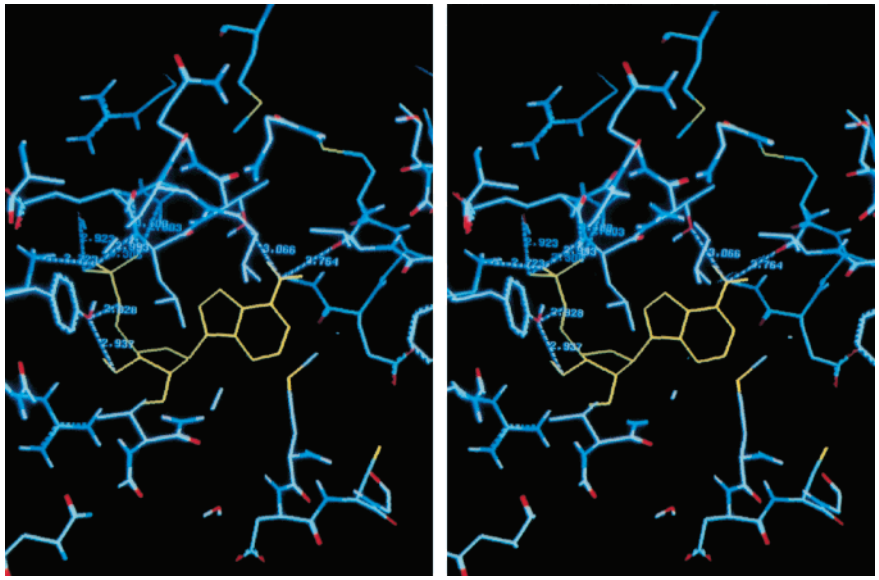

Figure 3. Stereoview of the allosteric binding site of fructose 1,6-bisphosphatase and the binding geometry of AMP (yellow).

than 15.0 Å or less than 2.5 Å away from any solute atoms were removed. Aqueous-phase dynamics simulations were carried out in a rectangular box using periodic boundary conditions in all directions. Newton's equations of motion for all of the atoms were solved using the Verlet algorithm[15] with a 2 fs time step. SHAKE[16] was used for constraining all bond lengths. Constant temperature (N, P & T ensemble) was maintained by velocity scaling all atoms in the system. Nonbonded interaction energies were calculated using a 15.0 Å residue-based cutoff.

For the protein complex simulations (the second cycle of Figure 2), it was necessary to first generate the hydrogen atom coordinates (for the all-atom force field to be applied), since they are not determined by X-ray crystallography. The EDIT module of AMBER was used to add hydrogens to the protein tetramer and the crystallographic waters. The protonation state of histidine was deduced from analysis of neighboring residues and from hydrogen-bonding potential. The total charge on the FBPase tetramer complex was +4 e. No counterions or changes in the customary charge of protein residues were used. The entire system was immersed in a 25.0 Å radius sphere of solvent centered around the mutating group. The water sphere was subjected to a half-harmonic restraint near the boundary to prevent evaporation. During the simulation, all atoms of the protein were fixed beyond 25.0 Å. All nonbonded interactions involving the inhibitors and the charged residues of the protein were computed with an infinite cutoff. A 15.0 Å nonbonded residue-based cutoff was used for other residues of the system. The algorithm for the complex simulation was identical to the solvent simulation except for the absence of periodic boundary conditions in the former.

X-ray Structure

The X-ray structure of the ZMP:human liver FBPase complex was solved at 2.3 Å resolution, refined using Xplor to the crystallographic *R* factor of 0.205, and made available to us by Professor W. Lipscomb (Harvard University). FBPase is a tetrameric molecule with four identical polypeptide chains (C1−C4). C1 and C2 comprise the crystallographic *n*-symmetric unit. Analysis of the X-ray structure of the FBPase−ZMP complex shows that there are slight differences between each subunit with regard to the atomic positions for several residues (e.g., Arg140 and Lys112 side chains) and the number and position of water molecules in the AMP binding site. Consequently, we calculated the interaction energy of ZMP in each subunit. The calculated interaction energies after energy minimization indicated that the C4 subunit had the lowest energy (C4 < C1 < C3 < C2). Accordingly, the C4 subunit was used for all molecular modeling calculations. AMP was overlayed on ZMP complexed to the C4 subunit. Figure 3 shows the stereoview of the binding-site geometry and the important hydrogen bonds formed between AMP and the FBPase binding-site residues.

Structural Comparison. The average "dynamical" structure of the FBPase−AMP complex was computed following energy minimization using 500 steps of steepest descent followed by 2000 steps of conjugate gradient and equilibration using a 20 ps MD simulation. For time steps of 1 and 2 fs in the MD simulations, the root-mean-square (RMS) deviations from the crystal structure were 1.10 and 1.17 Å for backbone atoms and 1.55 and 1.61 Å for side chain atoms, respectively. As expected, the largest deviations were observed on the surface (with RMS deviations of 1.28 and 1.70 Å for backbone and side chain atoms, respectively) when compared to the rest of the protein. This is primarily due to the flexibility of the protein at the protein−water interface. Since both time steps gave structures that are in good agreement with the X-ray structure, we used the larger time step, that is, 2 fs, for all of the free energy calculations to save computer time.

Results and Discussion

Validation of the FEP Methodology. The mutation of ZMP to AMP was performed to test the validity of our protocol. Since this mutation involves significant changes in ligand structure, the 'thread' method[10] was used to accomplish the transformation. Accordingly, the bases of ZMP and AMP were 'threaded' together at C1′. The calculated difference in binding free energy of 1.70 ± 0.9 kcal/mol is in good agreement with the experimentally measured free energy difference of 1.3 kcal/mol (Table 1). These results indicate that ZMP binds to FBPase

(15) Verlet, L. *Phys. Rev.* **1967**, *159*, 98−103.
(16) Ryckart, J. P.; Ciccotti, G.; Berendsen, H. J. C. *J. Comput. Phys.* **1977**, *23*, 327−341.

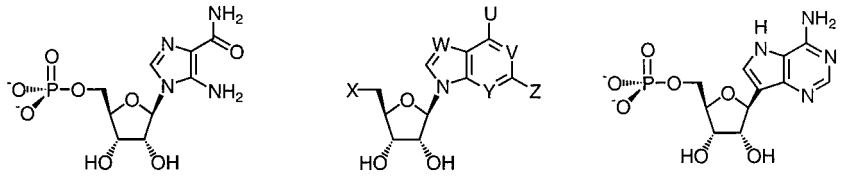

1 20

Compounds	X	Y	Z	V	U	W
2	$OPO_3^=$	N	H	N	NH_2	N
3	$CH_2PO_3^=$	N	H	N	NH_2	N
4	OSO_3^-	N	H	N	NH_2	N
5	CH_2COO^-	N	H	N	NH_2	N
6	$CH(COO^-)_2$	N	H	N	NH_2	N
7	$OPO_3^=$	N	SCH_3	N	NH_2	N
8	$OPO_3^=$	N	CH_3	N	NH_2	N
9	$OPO_3^=$	N	C_2H_6	N	NH_2	N
10	$OPO_3^=$	N	Cl	N	NH_2	N
11	$OPO_3^=$	N	H	CH	NH_2	N
12	$OPO_3^=$	CH	H	N	NH_2	N
13	$OPO_3^=$	CH	H	CH	NH_2	N
14	$OPO_3^=$	CH	H	CF	NH_2	N
15	$OPO_3^=$	CH	H	CC_2H_5	NH_2	N
16	$OPO_3^=$	N	H	N	H	N
17	$OPO_3^=$	N	H	N	CH_3	N
18	$OPO_3^=$	N	H	N	Cl	N
19	$OPO_3^=$	N	H	N	NH_2	CH

Figure 4. AMP analogues.

with lower affinity relative to AMP. The lower affinity is attributed in part to the higher desolvation free energy of ZMP (−1.5 kcal/mol), which presumably results from the increased number of hydrogen bonds formed between ZMP and water. In addition, ZMP is associated with increased conformational freedom (higher entropy) relative to AMP and therefore likely pays greater entropic costs.

Analysis of AMP Analogues

Scanning the AMP binding site of FBPase using the free energy perturbation method[5] indicated that hydrogen-bond interactions with the phosphate, 6-amino group, and N7 were important for high binding affinity. In addition, the scan revealed areas of AMP that contributed little to binding affinity. Using this information, we designed AMP analogues using structural modifications tailored for the AMP binding site. For example, new substituents were added to various positions of AMP to gain favorable interactions with binding site residues. In other cases, the groups deemed to be essential from the ligand scanning studies were replaced with structural mimetics designed to retain the binding site interactions but provide improved drug-like qualities.

Substitutions at the C5′ Position. Phosphates are often poor drug candidates[17] due to their instability in biological fluids and inability to penetrate cell membranes. As a result, we focused our initial efforts on the analysis of AMP analogues in which the phosphate was replaced with potential phosphate mimics (Figure 4). Calculations were carried out comparing the binding affinity of AMP with phosphonate (**3**), sulfate (**4**), carboxylate (**5**), and dicarboxylate (**6**). The double topology method was used for the mutation of AMP to carboxylate (**5**) and dicarboxylate (**6**) due to the large structural changes associated with these mutations. The single topology method was used for the mutation of AMP to phosphonate (**3**) and sulfate (**4**). The calculated relative differences in the solvation and binding free energies are reported in Table 1. The free energy differences between AMP and phosphonate (**3**) show that the phosphonate costs 1.0 kcal/mol less to desolvate than AMP. Despite the lower desolvation cost, phosphonate (**3**) was a significantly less potent FBPase inhibitor (3.9 kcal/mol). The large loss in relative binding affinity is likely due to the loss of the hydrogen bond between the 5′ oxygen and the phenolic hydroxyl of Tyr113. In addition, relative to phosphates, phosphonates are less acidic and consequently less charged, which likely decreases the interaction energy to the protein residues in the phosphate binding site.

Table 1. Calculated Relative Solvation and Binding Free Energies[a] between AMP and Its Analogs to FBPase (Units are in kcal/mol)

mutation	$\Delta\Delta G_{sol}$	$\Delta\Delta G_{bind(calc)}$	$\Delta\Delta G_{bind(expt)}$
AMP(**2**) → ZMP (**1**)	−1.5 ± 0.7	1.7 ± 0.9	1.3
AMP → phosphonate **3**	1.1 ± 0.6	4.6 ± 0.8	>5.5
AMP → adenosine 5′-sulfate (**4**)	NC[b]	3.5 ± 1.6	>2.6
AMP → carboxylate **5**	NC	5.0 ± 2.0	>3.6
AMP → dicarboxylate **6**	−2.3 ± 0.8	1.2 ± 0.9	ND[c]
AMP → 2-*S*-methyl AMP (**7**)	−1.6 ± 0.5	0.25 ± 0.6	0.3
AMP → 2-methyl AMP (**8**)	0.4 ± 0.4	0.20 ± 0.5	ND
AMP → 2-ethyl AMP (**9**)	0.5 ± 0.5	0.7 ± 0.6	1.0
AMP → 2-chloro AMP (**10**)	−0.9 ± 0.6	0.8 ± 0.7	1.1
AMP → 1-deaza AMP (**11**)	0.7 ± 0.4	−0.6 ± 0.5	ND
AMP → 3-deaza AMP (**12**)	1.1 ± 0.4	−0.5 ± 0.5	ND
AMP → 1,3-dideaza AMP (**13**)	1.3 ± 0.5	−0.8 ± 0.6	ND
AMP → 1,3-dideaza-1-fluoro AMP (**14**)	1.0 ± 0.6	−1.3 ± 0.7	ND
AMP → 1,3-dideaza-1-ethyl AMP (**15**)	1.2 ± 0.6	−0.5 ± 0.7	ND
AMP → PR[d] monophosphate (**16**)	4.0 ± 0.6	2.3 ± 0.8	2.7
AMP → 6-methyl PR monophosphate (**17**)	3.5 ± 0.7	2.0 ± 0.9	ND
AMP → 6-chloro PR monophosphate (**18**)	4.9 ± 0.6	1.2 ± 0.8	1.4
AMP → 7-deaza AMP (**19**)	0.8 ± 0.5	2.8 ± 0.6	3.3
AMP → formycin monophosphate (**20**)	0.5 ± 0.4	0.6 ± 0.5	0.3

[a] Free energies are relative to AMP. [b] NC = not calculated. [c] ND = not determined. [d] PR is purine riboside.

The calculated relative binding free energies for sulfate (**4**) and carboxylate (**5**) relative to AMP are 3.5 ± 0.6 and 5.0 ± 1.6 kcal/mol, respectively. These calculated free energies are qualitatively similar to the experimental results of >2.6 and >3.6 kcal/mol. The large change in charge between the phosphate (−2e) and either the carboxylate or sulfate (−1e) is likely to

(17) Starrett, J. E.; Tortolani, D. R.; Hitchcock, M. J.; Martin, J. C.; Mansuri, M. M. *Antiviral Res.* **1992**, *19*, 267.

account for the reduced binding affinity. This change in charge is commonly associated with a decrease in accuracy in free energy calculations. Nevertheless, the qualitative trend was correctly predicted. Analysis of the calculated relative solvation and binding free energies between dicarboxylate (**6**) and AMP showed that the dicarboxylate (**6**) costs 2.3 kcal/mol more to desolvate but gains about 1.1 kcal/mol in the complex as compared to AMP. Accordingly, the dicarboxylate analog (**6**) binds less effectively (1.2 kcal/mol) to FBPase, even though it gained favorable interactions in the binding-site residues relative to AMP. On the basis of the calculated relative binding free energies none of the four phosphate mimics were predicted to bind to FBPase as effectively as phosphate.

Substitutions on the Pyrimidine Ring. The pyrimidine ring of AMP was modified on the basis of a graphical analysis of the FBPase−AMP binding site (Figure 3). The X-ray structure of the FBPase−AMP complex revealed unfilled space near N1, C2, and N3. Since the residues in the vicinity were hydrophobic and neither N1 nor N3 participated in a hydrogen bond with the protein, analogues, 2-*S*-methyl AMP (**7**), 2-methyl AMP (**8**), 2-ethyl AMP (**9**), and 2-chloro AMP (**10**) (Figure 4) were evaluated to determine whether these substituents gained favorable hydrophobic interactions with Met 188. The calculated free energies shown in Table 1 indicate that relative to AMP, 2-methyl AMP and 2-ethyl AMP were predicted to be slightly weaker FBPase inhibitors despite their reduced desolvation costs. The rationale for the decreased binding affinity in the complex was not apparent from analysis of the X-ray structure but the results were consistent with the inhibition potency determined subsequently for compound **9**. In comparison, 2-*S*-methyl AMP and 2-chloro AMP showed a gain in the complex free energy. However, consistent with the experimental results, these analogues were also weaker FBPase inhibitors than AMP presumably because of the large increase in desolvation costs predicted to occur with these substituents.

In addition to the 2-substituted analogues, several deaza AMP analogues were evaluated to determine whether the expected reduction in desolvation costs produced by the base modification would result in an AMP analogue with enhanced binding affinity. Since each mutation between AMP and the pyrimidine ring analogues (**11**−**15**) involved relatively minor changes in the inhibitor structures, we used a single topology for the reactant and product molecules. As expected 1-deaza AMP (0.7 kcal/mol), 3-deaza AMP (1.1 kcal/mol), 1,3-dideaza AMP (1.3 kcal/mol), 1,3-dideaza-1-fluoro AMP (1.0 kcal/mol), 1,3-dideaza-1-ethyl AMP (1.2 kcal/mol) showed decreased desolvation costs and improved binding affinity (Table 1) to FBPase as compared to AMP.

The X-ray structure of FBPase complexed with AMP (Figure 3) showed hydrogen bonds between the 6-amino group of AMP with both the side chain hydroxyl of Thr 31 and the backbone carbonyl oxygen of Val17. In addition, N7 appeared to be within hydrogen-bonding distance to the hydroxyl group of Thr31. To understand the binding affinity contribution of the hydrogen bonds formed between the 6-amino group and FBPase, purine riboside monophosphate (**16**), 6-methyl purine riboside monophosphate (**17**), and 6-chloro purine riboside monophosphate (**18**) were evaluated using the single topology and FEP method. The calculated relative solvation and binding free energies are shown in Table 1 with the latter results showing good agreement with available experimental data. The observed binding preference of AMP relative to the 6-desamino AMP analogues (**16**−**18**) is attributed to the two strong hydrogen bonds formed with the 6-amino group and the large favorable interaction energy which appears to more than offset the large desolvation penalty associated with the amino group.

Imidazole Ring Modifications. 7-Deaza AMP (**19**) and formycin monophosphate (**20**) (Figure 4) were evaluated to assess whether AMP analogues lacking N7 or using N7 as a hydrogen-bond donor were suitable FBPase inhibitors. The results from our FEP calculations using a single topology are reported Table 1. Relative to AMP, the desolvation gain for 7-deaza AMP (**19**) is about 0.8 kcal/mol. Apparently, however, the loss of the N7 hydrogen bond to the hydroxyl of Thr31 residue results in a 2.8 kcal/mol loss in binding affinity compared to AMP.

The major difference between AMP and formycin monophosphate (**20**) is that the N7 of formycin acts as a hydrogen-bond donor, whereas the N7 in AMP acts as a hydrogen-bond acceptor. Despite this significant structural change and the earlier results with 7-deaza AMP showing that N7 interaction is very important for high binding affinity, the mutation of AMP to formycin (**20**) led to a relative free energy difference of only 0.6 kcal/mol. The graphical analysis following 20 ps of MD simulation showed that the FBPase binding site accommodated the change in the N7 hydrogen bond characteristics by a slight rearrangement in the nearby binding-site residues, especially the Thr31 side chain. Overall, both compounds showed a similar number of hydrogen bonds in the complex as in solvent. The calculated relative binding free energy indicates that the small loss of free energy in the solvent for AMP is compensated for in the complex by slightly more favorable interactions with the protein**.** The changes in free energy, both in the solvent and in the complex, could be due to the loss of an intramolecular hydrogen bond between N7 and the 6-amino group and a change in the geometry of the 6-amino group. The net result is that the calculations supported the experimental results showing that despite a large difference in hydrogen-bond potential, formycin monophosphate is an FBPase inhibitor with a potency only slightly less than that of AMP.

Conclusions

A successful application of a computer-assisted drug design paradigm is described in this article using the FEP approach as a means to accurately predict the FBPase inhibitor SAR of AMP analogues. Accurate prediction of inhibitor SAR is expected to shorten the time required to find suitable candidates for drug development by eliminating the time expended on the synthesis and characterization of compounds that ultimately prove to be weak inhibitors and by focusing chemistry efforts on more promising compound series. In our studies, the calculated results were consistent with experimental data. This study also elucidated the importance of solvation free energy in the binding of AMP analogues to FBPase. In some cases, desolvation energy costs significantly reduced binding affinity, while in other cases the group associated with the high desolvation energy also formed strong favorable interactions with the protein which more than compensated for the desolvation costs and therefore led to an improvement in relative binding affinity. Except for the FEP method, which is very expensive computationally and cannot be used for all proposed analogues of a lead compound, no other computation method provides accurate solvation free energies. These results support the use of the FEP methodology in the drug design process as a means to generate SAR information and important insights into the factors controlling inhibitor binding affinity.

Acknowledgment. We thank Drs. H. M. Ke, Y. P. Zhang, and William Lipscomb (Harvard University) for human FBPase

crystallographic data, Dr. Paul van Poelje and Mr. Juergen Schanzer for determining the FBPase inhibition constants and Drs. Max Dang, Gerard Scarlato, and Kurt Metzner for synthesizing some of the FBPase inhibitors.

Supporting Information Available: Parameters and partial atomic charges for all the inhibitors (Table 1), and calculated relative gas, aqueous and complex free energies between AMP and its analogues (Table 2) (PDF). This material is available free of charge via the Internet at http://pubs.acs.org.

JA0103288